^{1}H and ^{2}H NMR Spin−Lattice Relaxation Probing Water: PEG Molecular Dynamics in Solution

Eduardo M. Clop,[†] María A. Perillo,[†] and Ana K. Chattah*[,‡]

[†]Instituto de Investigaciones Biológicas y Tecnológicas (IIByT), CONICET - Facultad de Ciencias Exactas Físicas y Naturales, Universidad Nacional de Córdoba, Av. Vélez Sarsfield 1611, X5016GCA Córdoba, Argentina

[‡]Facultad de Matemática Astronomía y Física, Universidad Nacional de Córdoba, IFEG-CONICET, X5016LAE Córdoba, Argentina

ABSTRACT: Nuclear magnetic resonance spin−lattice relaxation times (T_1) measurements were performed in aqueous solutions of poly(ethylene glycol) (PEG) of 6000 Da molecular mass to study the dynamical relation between PEG and water molecules at different solute concentrations. ^{1}H−T_1 experiments were carried on at a low magnetic field in the time domain (20 MHz) and at a high field (400 MHz) to obtain spectral resolution. Two contributing components were identified in each proton system, PEG and water, presenting values of T_1 with very different orders of magnitude. The approximate matching between the shorter ^{1}H−T_1 values associated with water and PEG has lead us to conclude that there exists a network of interactions (hydrogen bonds) between the solute and the solvent, which results in the presence of an ordered and dehydrated structure of PEG folded or self-assembled in equilibrium with a more flexible monomer structure. Dynamic light scattering results were consistent with the formation of PEG aggregates, showing a mean size between 40 and 100 nm.
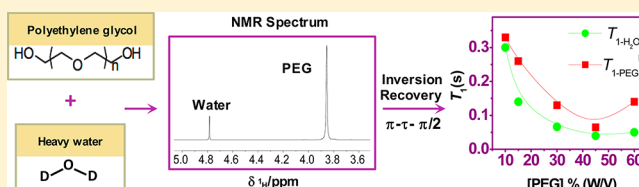
INTRODUCTION

A crowded environment is a system where macromolecules occupy large volume fractions that cannot be taken up by other molecules. These systems include 3D networks where molecules that are large if compared with pore size are confined.[1,2] As a result, the molecules are submitted to steric and diffusional restrictions affecting their properties.[3] In a molecular crowded environment, contrary to what happens in a dilute aqueous solution, the thermodynamic activity of the macromolecules increases by several orders of magnitude,[4,5] the diffusion rates of molecules are reduced, and the solvent becomes structured due to the supply of large surfaces, where it can be immobilized by adsorption. This phenomenon can affect the folding of proteins[4,5] and, consequently, their activities (e.g., enzymatic activity).[6] The structure of water can also modify the affinity of the enzyme−substrate hydrophobic interaction and thus affect enzymatic reaction kinetics. Consequently, the effect of molecular crowding on biochemical reaction rates is complex because although the diffusion rate decreases the thermodynamic activity of the components increases. The final outcome will depend on the nature of the reaction.[1,2]

Crowding agents should be added to the solution to simulate macromolecular crowding in vitro. The most commonly used crowding agents are bovine serum albumin (BSA), ovalbumin, Ficoll 70, and poly(ethylene glycol) (PEG).[7]

The addition of known amounts of a crowded agent to a biochemical reaction media is helpful to study, in controlled conditions, the concept of water structure and dynamics as well as its significance on the whole molecular system. Liquid water is a macroscopic network of molecules connected by hydrogen bonds in continuous topological reformation.[8] Ions in solution,

hydrophilic residues, and small molecules can be immobilized by water molecules through hydrogen bonds contributing to a nonfreezable water component, as it is called from the differential scanning calorimetry standpoint. Because of this diversity of interactions, it is possible to describe the water in solutions as a set of dynamic subsystems defined by a spectrum of binding energies of water molecules adsorbed to different sites at macromolecules.[9]

Nuclear magnetic resonance (NMR) through spin−lattice and spin−spin relaxation times has proven to be a very useful technique to provide information on aqueous solutions on a variety of time scales and solute concentrations.[10−17] In particular, allowing to identify the dynamics of different water distributions and helping to distinguish free liquid fractions from structured water in the presence of solutes.[18,19] In addition, it is a noninvasive method that can be applied to a wide spectrum of solution samples.

In this work, the dynamic behavior of both water and PEG in H$_2$O/PEG solutions at different PEG concentrations was studied performing NMR experiments, in particular, measuring proton (^{1}H) and deuterium (^{2}H) spin−lattice relaxation times (T_1). Dynamic light scattering experiments have been performed to complement our NMR analysis and to give support to our conclusions.

H$_2$O/PEG solution is a system widely studied by experimental techniques including NMR, computational dynamics, and, recently, dynamic light scattering, fluorescence

spectroscopy, and surface tension measurements.[20−28] Our analysis provides a new approach to the understanding of the system, finding a close relation between the dynamics of PEG and water.

■ EXPERIMENTAL SECTION

Materials. PEG 6000 was purchased from Droguerias Saporiti (Parafarm). Virgin deuterated water was kindly donated by Central Nuclear Embalse de Río Tercero, Córdoba, Argentina. H_2O/PEG solutions were prepared at PEG concentrations ([PEG]) ranging between 0 and 70% W/V, providing systems from dilute to highly concentrated levels. The temperature was set to 37 °C in all experiments to emulate biochemical conditions.

Nuclear Magnetic Resonance. Spin−lattice relaxation times (T_1) were measured using the inversion recovery (IR) pulse sequence (π-t-π/2-Acquisition).[29]

A Bruker-Minispec (20 MHz) was used to perform $^1H−T_1$ experiments, measuring the amplitude of the free induction decay (FID) as a function of t. In this case, $\pi/2$ was calibrated to 2.6 μs, and t varied within 1 ms and 18 s. In a Bruker Avance 400 MHz, a second set of $^1H−T_1$ experiments was done to obtain spectral resolution. In this case, solutions were prepared with PEG dissolved in D_2O, containing trace amounts of H_2O. Then, two separated resonances belonging to PEG and H_2O were observed. The recovery times t ranged between 1 ms and 120 s. Each peak was integrated separately to obtain the magnetization as a function of t. $^2H−T_1$ measurements in D_2O/PEG solutions were done in a Bruker Avance 300 MHz. Here the recovery times took values within the range of 10 μs ≤ t ≤ 2 s.

In our IR experiments, proton or deuterium magnetization $M(t)$ follows a two-exponential behavior

$$M(t) = M_0(1 - 2*A*\exp(-t/T_1^a) - 2*(1 - A)$$
$$*\exp(-t/T_1^b)) \tag{1}$$

as the magnetization has been normalized, that is, $M_0 = 1$, the parameters A and $(1 − A)$ can be directly interpreted as the proportions of the whole sample exhibiting T_1^a and T_1^b, respectively. In the case $A = 1$, the fitted function resulted monoexponential, exhibiting only one relaxation time.

Dynamic Light Scattering (DLS). H_2O/PEG solutions at different concentrations were introduced into the thermostatized sample cell of a Nicomp model 380 submicrometer particle sizer (PSS, CA) using a 632.8 nm laser source with an angle of 90°. Each sample was measured at least twice for 10 min each. The solvent (Milli-Q water) was filtrated through 0.2 μm pore size PVDF filter (Millipore) to avoid contamination. Data were collected and analyzed with the software provided with the instrument, which utilizes the NICOMP algorithm for diameter calculations. The channel width was automatically set by the instrument, and the refraction index and viscosity of each solution were obtained from literature.

■ RESULTS AND DISCUSSION

Figure 1 displays the $^1H−T_1$ values obtained in H_2O/PEG solutions as a function of PEG concentration in the measurements at 20 MHz. The best fittings to $M(t)$ were obtained using eq 1. Figure 1 shows the presence of two components for each concentration that behave notably different: one component with a long relaxation time (0.55 < T_1^a < 3 s) and another component presenting a short time (T_1^b
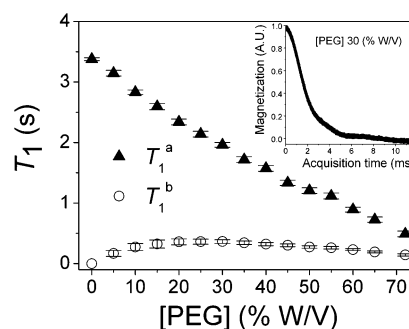

Figure 1. ^1H spin−lattice relaxation times, T_1^a (▲) and T_1^b (○) obtained in H_2O/PEG solutions as a function of [PEG]. The values are obtained by fitting a two-exponential function to $M(t)$ in the IR experiment at 20 MHz. Error bars are displayed. Inset: FID recorded at 30% W/V, showing the typical decay for an homogeneous solution.

< 0.4 s). Note that T_1^a decreased with PEG concentration, which is in agreement with the behavior of a solution with increasing viscosity.[29,30] T_1^b showed a little increment at low concentrations and then, it remained barely constant. Note that data for $M(t)$ belong to the interfering signal of all protons present in the sample, those becoming from water and from PEG, respectively. The recorded FID showed a smooth Gaussian-like decay (see inset in Figure 1), making the possibility to identify the presence of two components difficult. This homogeneity of the FID was attributed to the liquid character of the system, where no different macroscopic phases coexist. This fact differs from the behavior reported in a gelatin/water system, where it was possible to distinguish two components directly from the FID measured at 20 MHz, at different protein concentrations.[10] In that case, the fast component of the FID was associated with the more solid part belonging to gelatin protons, where the slow decay was associated with protons belonging to hydration water together with extremities of gelatin chains.

Figure 2 shows the proportion of protons associated with T_1^a obtained from the fittings of eq 1 to $M(t)$ as a function of
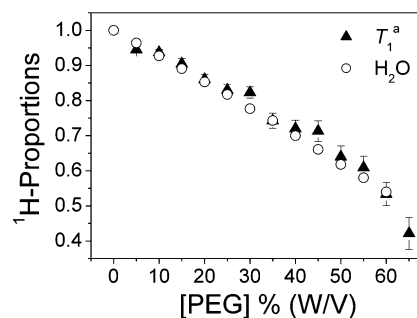

Figure 2. Proportions of ^1H belonging to water in H_2O/PEG solution calculated from the amount of water added to the mixture (○), in approximate coincidence with the ^1H proportion associated to T_1^a (IR experiments at 20 MHz) (▲). Error bars are shown.

[PEG]. In addition, the proportion of protons belonging to water is observed, calculated with the amount of water added to the mixture. The coincident behavior of these two proportions was indicative that T_1^a component can be assigned to water protons. Thus, T_1^b might be associated with PEG protons. The absence of a component with a relaxation time characteristic of pure water (3.5 s at 20 MHz), even at low PEG concentrations,

shows that the solution is being affected by the polymer on all scales.

This conclusion is supported by the fact that an evidence of a discrete structured water fraction, different from bulk water, was not obtained with these experimental settings. Moreover, it is interesting to note that T_1^a approximates to T_1^b at high polymer concentrations, showing that almost all water tends to interact with PEG molecules.

It is important to remark that in our experiments fixing a characteristic time for the bulk water component and letting the other parameters free in a multiexponential equation for $M(t)$ did not lead to good fitting results. Then, our analysis differs from reported experiments performed in similar systems.[12]

To obtain resolved information, $^1H-T_1$ values of D_2O/PEG solutions containing trace amounts of H_2O, were measured at 400 MHz. Figure 3 shows the ^1H spectrum of a solution
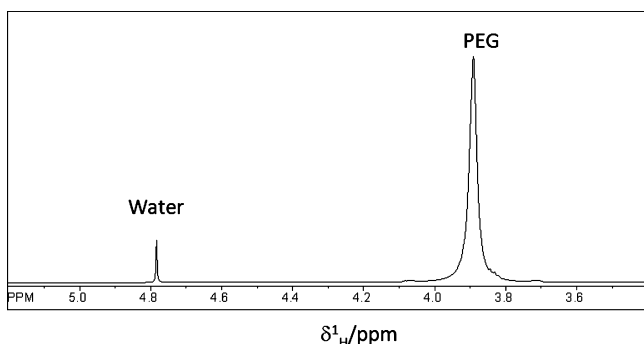

Figure 3. ^1H NMR spectrum of D_2O/PEG solution at 30%W/V showing the residual H_2O/DOH peak.

containing 30% W/V of PEG. The two resonances observed were assigned to PEG and H_2O. For all concentrations, each peak was integrated separately to obtain the ^1H magnetization for PEG and H_2O as a function of t, $M_{PEG}(t)$, and $M_{H_2O}(t)$. These $M(t)$ curves were best fitted to eq 1 showing the presence of two components for all the concentrations, both in water and in PEG. In water, the major component presented a long T_1 ($T_{1-H_2O}^a \cong 20$ s) that decreased with [PEG] in accordance with the behavior observed in the experiments at low field. (See Figure 4a.) In addition, it was observed a second component with shorter T_1 values ($T_{1-H_2O}^b \cong 0.06$ to 0.3 s). Surprisingly, $M_{PEG}(t)$ also showed two components (Figure 4b). The component with the highest proportion was characterized by short relaxation times ($T_{1-PEG}^b \cong 0.05$ to 0.3 s,), and the second component showed longer values ($T_{1-PEG}^a \cong 0.8$ to 1.45 s).

A common approach to address relaxation times measurements in dilute solutions is the fast exchange model between two water components (bound and unbound), as it has been applied to aqueous solutions of PEG[21,22] or cyclodextrins.[11] In our case, a different approach is used, exploring the possibility of directly obtaining two relaxation times from the ^1H magnetization, a major contributing component and a second one with a very small population.[11,22]

Table 1 summarizes the relaxation times and population proportions obtained by fitting a two-exponential behavior to $M_{PEG}(t)$ and $M_{H_2O}(t)$. It is interesting to note that T_{1-PEG}^b and $T_{1-H_2O}^b$ presented values within the same order of magnitude. (See Figure 5.) This lead us to conclude that there is a

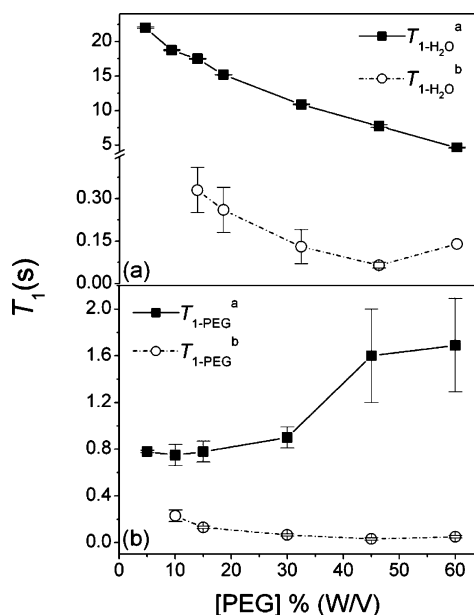**Figure 4.** (a) ^1H relaxation times $T_{1-H_2O}^a$ (■) and $T_{1-H_2O}^b$ (○) obtained as a function of [PEG] by fitting a two-exponential function to the water magnetization ($M_{H_2O}(t)$). (b) ^1H relaxation times T_{1-PEG}^a (■) and T_{1-PEG}^b (○) obtained as a function of [PEG] by fitting a two-exponential function to the PEG magnetization $M_{PEG}(t)$.

population of PEG strongly interacting with a component of water, producing the homogenization of the relaxation times. The long relaxation time for water $T_{1-H_2O}^a$ decays with PEG concentration, which is in accordance with liquid systems of increasing viscosity. The observed increase in T_{1-PEG}^a as a function of [PEG] is indicative that this component behaves as a solid, where the increment in the concentration produces higher rotational correlation times.[29]

The proportions of protons P_{PEG}^b and $P_{H_2O}^b$ associated with the short T_1 values (Table 1) increase with [PEG], indicating that the presence of more polymer molecules favors the formation of a more rigid network. In fact, the increase in P_{PEG}^b would be favored by the growing interaction energy among PEG molecules, accompanying the increase in its thermodynamic activity. The complementary proportions (belonging to the long T_1 values) are calculated as $1 - P^b$. Note that $P_{H_2O}^b$ is the smallest component ($\ll 1$), whereas P_{PEG}^b is the major component in the case of the polymer. The proportions P_{PEG}^b and $P_{H_2O}^b$ were used to calculate the number of immobilized water molecules per monomer of immobilized PEG. The number of immobilized water molecules per monomer always resulted below 1 (see Table 1), whereas values between 1 and 4 have been reported in the literature.[21] The fact that the ratio $P_{H_2O}^b/P_{PEG}^b$ is significantly smaller than $P_{H_2O}^a/P_{PEG}^a$ (much less immobilized water than immobilized PEG) indicates that the immobilized PEG conformer presents a more compact and dehydrated structure in comparison with the more mobile one. Then, the presence of a more dehydrated core (hydrophobic) would explain the smaller number of immobilized water molecules per monomer subunit. The number of H_2O molecules per monomer subunit (Table 1, last column) of the more free components (T_{1-PEG}^a and $T_{1-H_2O}^a$) was also calculated. Considering the lack of a population with bulk

Table 1. ^{1}H−T_1 Values and Corresponding Proportions Obtained from a Two-Exponential Fitting Function to the Magnetization $M_{PEG}(t)$ and $M_{H_2O}(t)$ in the IR Experiments at 400 MHz^a

[PEG] (%W/V)	$T_{1-H_2O}^a$ (s)	$T_{1-H_2O}^b$ (s)	$P_{H_2O}^b$	T_{1-PEG}^a (s)	T_{1-PEG}^b (s)	P_{PEG}^b	$P_{H_2O\ molec}^b/P_{PEG\ mon}^b$	$P_{H_2O\ molec}^a/P_{PEG\ mon}^a$
0	22							
5	18.7			0.78				
10	17.5	0.33	0.003	0.89	0.3	0.60	0.13	64
15	15.2	0.26	0.010	0.91	0.14	0.84	0.19	101
30	10.9	0.13	0.026	0.98	0.07	0.90	0.20	68
45	7.7	0.06	0.025	1.30	0.04	0.85	0.12	25
60	4.6	0.14	0.120	1.40	0.05	0.86	0.33	15

^{a}Proportions of ^{1}H associated with the short T_1 values are shown ($P_{H_2O}^b$ and P_{PEG}^b). These proportions were used to calculate the number of immobilized water molecules per monomer unit of the less-mobile PEG (penultimate column) and the number of more free water molecules per monomer in the more mobile PEG (last column). Errors are within 7% (for $T_{1-H_2O}^a$ and T_{1-PEG}^b) and 15% (for $T_{1-H_2O}^b$ and T_{1-PEG}^a). Subscripts molec and mon refer to molecules and monomer units, respectively.
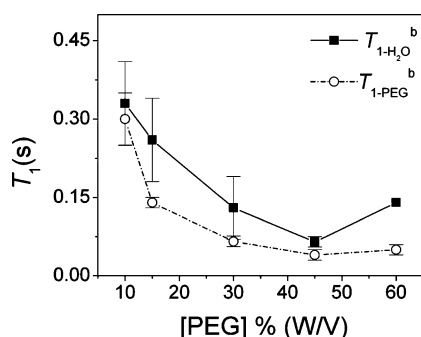
Figure 5. Comparison of $T_{1-H_2O}^b$ (■) and T_{1-PEG}^b (○) versus [PEG], showing an approximate matching between them.

water, we can assume that all water molecules with $T_{1-H_2O}^a$ are being affected by the PEG monomers having T_{1-PEG}^a. These results showed that a very high number of water molecules are interacting with the polymer in the more flexible conformation, affecting globally the whole hydrogen bond network of water in the solution.

Our results indicated that both the solute (PEG) and the solvent (water) showed two populations with different degree of order. Both PEG populations could be explained either by an equilibrium between two molecular conformations or by the presence of supramolecular aggregates of PEG molecules. Aggregation of poly(ethylene oxide) (PEO) in solution has been confirmed by light scattering, electron microscopy, viscometry, calorimetric techniques, and sedimentation velocities.[31,32] The formation of PEO clusters has been found to be dependent on the solvent type, the temperature, and the polymer solution concentration. It was found that above a critical self-association concentration, which depends on the molecular weight of the PEO, polymer clusters and free polymer coils coexist in a thermodynamic equilibrium.[31,33] However, the direct comparison between PEG and PEO is not correct due to the different functional groups present at the end of PEO chains (−CH$_3$) with respect to PEG (−OH), which can play a significant role in the stabilization of the self-assembled structures of each polymer. Even so, aggregate formation in H$_2$O/PEG solutions, using PEG of low molecular weight, has been recently observed through fluorescence spectroscopy and surface-tension measurements.[20,26]

The coexistence of two molecular conformations may be proposed as an alternative hypothesis to explain our results. Computational simulations based on molecular dynamics using

PEG of low molecular mass (up to 3400 Da) have been reported.[23−25] The coexistence between two conformers has been observed, showing the presence of an equilibrium between a more ordered helical form in opposite to a more disordered hydrated unfolded form.[34] In our case, the fact that the shorter T_1 corresponding to water and PEG has similar values may be suggesting that the immobilization of water stabilizes one of the PEG conformers. However, in numerical simulations, interactions between polymer molecules at high concentrations would be difficult to achieve.

The DLS experiments were made in a wide range of PEG concentrations between 0 and 60% W/V. PEG aggregates were evidenced at all concentrations studied. The NICOMP analysis gives access to three diameter distributions based on scattering intensity, sample volume, and particle number. In Figure 6a,b,
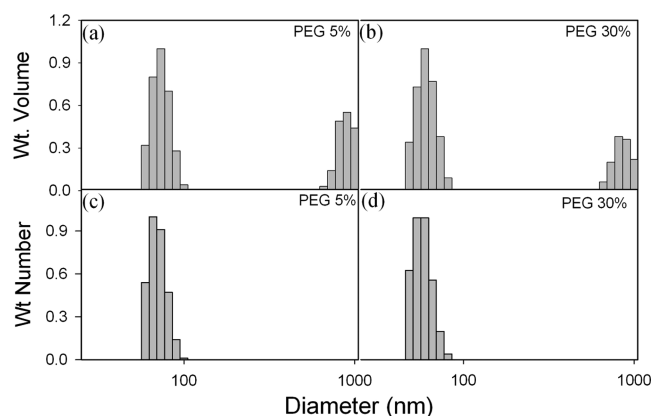
Figure 6. Size distribution obtained from DLS of H$_2$O/PEG solutions showing the weighted sample volume for concentrations (a) [PEG] = 5% W/V and (b) [PEG] = 30% W/V, where apparent bimodal distribution can be seen. The size distribution based on the weighted number of particles is examined for (c) [PEG] = 5% W/V and (d) [PEG] = 30% W/V.

the size distribution based on weighted sample volume is shown. There, a bimodal distribution is clearly observed at the two concentrations chosen as examples, corresponding to 5 (Figure 6a) and 30% PEG W/V (Figure 6b). This pattern is repeated at all concentrations studied. The population with the smallest diameter is clearly the more abundant one, having a mean diameter that varied between 40 and 90 nm, depending on [PEG]. This fact is in agreement with the formation of PEG aggregates, taking into account the fact that a PEG molecule of

6000 Da, has a radius of gyration of 3.1 nm given by R_g = $0.02M_p^{0.58}$ (nm).[35] Note that there is a second population presenting a larger mean diameter with values between 300 and 1000 nm (limit of DLS sensitivity). Figure 6c,d show the diameter distribution based on the number of particles. In that case, the small aggregates distribution appears as a sole population. This may be because bigger aggregates have a low number of particles to be fitted by the program. Figure 7
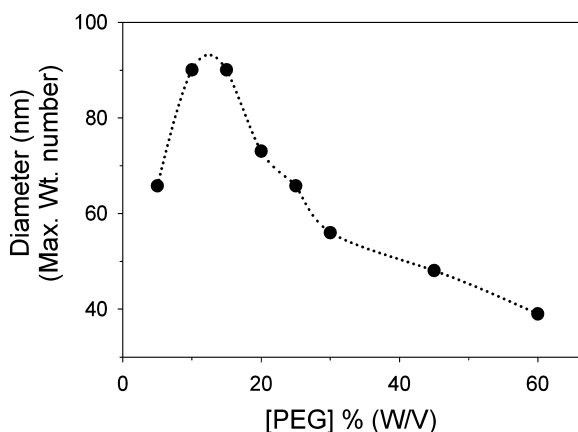

Figure 7. Diameter of the aggregates as a function of [PEG], obtained by picking the maximum value of the size distribution pattern.

shows the diameter as a function of [PEG], corresponding to the maximum of the distribution based on number of particles. The size of the aggregates does not exceed 100 nm, showing a maximum at ~15% W/V. PEG aggregates have been recently investigated by DLS.[28]

Our NMR experiments showed the presence of two PEG populations with different relaxation times. The population with the shorter longitudinal relaxation time implies an increment in the spin network size with strong interactions between PEG molecules. That behavior is consistent with the presence of the aggregates shown by DLS experiments, indicating that NMR experiments is sensing the dynamics of both the single PEG molecule and the PEG in aggregates.

Figure 8 displays $^2H-T_1$ values as a function of PEG concentration. The D_2O spectrum showed uniformity for all concentrations studied and absence of quadrupolar splitting. The deuterium magnetization as a function of t was well-fitted to a single-exponential behavior, leading to the relaxation time $T_{1\text{-}D_2O}$ (spin−lattice relaxation time of deuterium nuclei). It was
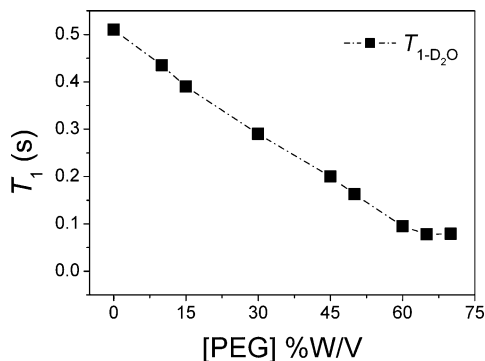

Figure 8. ^2H spin−lattice relaxation times, $T_{1\text{-}D_2O}$ as a function of [PEG].

possible to observe a monotonous decrease in $T_{1\text{-}D_2O}$ with [PEG]. This behavior was previously reported in the literature for PEO solutions within the same concentration range as that used for PEG in the present work,[21] whereas higher concentrations (that were not tested here) showed non-homogeneous behavior. We considered not achieving higher concentrations because they were not relevant for simulating molecular crowding conditions. The fact that in ^2H experiments a second population of deuterated water was not evident may be explained by observing that the order of magnitude for $^2H-T_1$ was ~40 times smaller than $^1H-T_1$ values. Because the detected T_1 for deuterium nuclei was on the order of milliseconds, it can be concluded that the second T_1 population may have been too short to be detected. A second component measuring ^2D spectrum has been observed at higher concentrations for a similar polymer.[21]

■ CONCLUSIONS

In this work, we have performed NMR spin−lattice relaxation times measurements in aqueous solutions of high-molecular-weight PEG (6000 Da) at different concentrations, from dilute to highly concentrated systems. Our aim was to study the dynamical behavior of both the solute and the solvent to understand the internal interactions between both components.

In the NMR experiments with spectral resolution, a separated analysis for water and PEG gave rise to a two-exponential recovery of the magnetization in each component. The close relation between the shorter relaxation time values of PEG and water for all concentrations was consistent with the presence of an ordered and dehydrated structure of PEG, folded or self-assembled, in equilibrium with a more flexible monomer structure with the ability to affect the global hydrogen bond network of the entire aqueous solution. The last statement was supported by DLS experiments, showing the presence of aggregates in the solution, indicating that the two populations of PEG observed in the NMR dynamics experiments could be sensing the dynamics of PEG both as a single molecule in solution and as forming part of an aggregate.

The aqueous solutions of PEG were used here as model systems to test the sensitivity of the NMR technique and, in particular, relaxation time experiments, to study water dynamics in a macromolecular crowded media, and to expand this analysis to more complex systems involving lipid aggregates grafted with PEG covalently bound at the lipid−water interface.

■ AUTHOR INFORMATION

Corresponding Author

*Phone: + 54-351-4334051 (ext. 369). Fax: + 54-351-4334054. E-mail: chattah@famaf.unc.edu.ar.

Notes

The authors declare no competing financial interest.

■ REFERENCES

(1) Ellis, R. J. *Curr Opin Struct Biol* **2001**, *11*, 114.
(2) Ellis, R. J. *Trends Biochem. Sci.* **2001**, *26*, 597.

(3) Hall, D.; Minton, A. P. *Biochim. Biophys. Acta* **2003**, *1649*, 127.

(4) Minton, A. P. *Mol. Cell. Biochem.* **1983**, *55*, 119.

(5) Zimmerman, S. B.; Minton, A. P. *Annu. Rev. Biophys. Biomol. Struct.* **1993**, *22*, 27.

(6) Matsue, S.; Miyawaki, O. *Enzyme Microb. Technol.* **2000**, *26*, 342.

(7) Chebotareva, N. A.; Kurganov, B. I.; Livanova, N. B. *Biochemistry (Moscow)* **2004**, *69*, 1239.

(8) Stillinger, F. H. *Science* **1980**, *209*, 451.

(9) Lamisovsky, D. R.; Schürrer, C. A.; Brunetti, A. H. *Appl. Magn. Reson.* **1996**, *12*, 61.

(10) Vackier, M.-C.; Hills, B. P.; Rutledge, D. N. *J. Magn. Reson.* **1999**, *138*, 36.

(11) Sabadini, E.; Egidio, F. d. C.; Fujiwara, F. Y.; Cosgrove, T. *J. Phys. Chem. B* **2008**, *112*, 3328.

(12) Kuentz, M.; Rothenhäusler, B.; Röthlisberger, D. *Drug Dev. Ind. Pharm.* **2006**, *32*, 1165.

(13) Lamisovsky, D. R.; Schürrer, C. A.; Brunetti, A. H. *Appl. Magn. Reson.* **1997**, *12*, 61.

(14) Arnulphi, C.; Martin, C. A.; Fidelio, G. D. *Mol. Membr. Biol.* **2003**, *20*, 319.

(15) Mears, S. J.; Cosgrove, T.; Thompson, L.; Howell, I. *Langmuir* **1998**, *14*, 997.

(16) Demangeat, J.-L. *J. Mol. Liq.* **2009**, *144*, 32.

(17) Fabri, D.; Williams, M. A.; Halstead, T. K. *Carbohydr. Res.* **2005**, *340*, 889.

(18) Wilkinson, D. A.; Morowitz, H. J.; Prestegard, J. H. *Biophys. J.* **1977**, *20*, 169.

(19) Chavez, F. V.; Schonhoff, M. *J. Chem. Phys.* **2007**, *126*, 104705.

(20) Derkaoui, N.; Said, S. r.; Grohens, Y.; Olier, R.; Privat, M. *J. Colloid Interface Sci.* **2007**, *305*, 330.

(21) Lüsse, S.; Arnold, K. *Macromolecules* **1996**, *29*, 4251.

(22) Ling, G. N.; Murphy, R. C. *Physiol. Chem. Phys. Med. NMR* **1983**, *15*, 137.

(23) Lee, H.; Venable, R. M.; Mackerell, A. D., Jr.; Pastor, R. W. *Biophys. J.* **2008**, *95*, 1590.

(24) Lee, H.; de Vries, A. H.; Marrink, S. J.; Pastor, R. W. *J Phys Chem B* **2009**, *113*, 13186.

(25) Smith, G. D.; Bedrov, D.; Borodin, O. *Phys. Rev. Lett.* **2000**, *85*, 5583.

(26) Azri, A.; Giamarchi, P.; Grohens, Y.; Olier, R.; Privat, M. *J. Colloid Interface Sci.* **2012**, *379*, 14.

(27) Hey, M. J.; Ilett, S. M.; Mortimer, M.; Oates, G. *J. Chem. Soc., Faraday Trans.* **1990**, *86*, 2673.

(28) Linegar, K. L.; Adeniran, A. E.; Kostko, A. F.; Anisimov, M. A. *Colloid J.*; MAIK Nauka/Interperiodica distributed exclusively by Springer Science+Business Media LLC; 2010; Vol. 72, p 279.

(29) Harris, R. *Nuclear Magnetic Resonance Spectroscopy*; Longman Scientific and Technical: Essex, England, 1994.

(30) Abragam, A. *The Principles of Nuclear Magnetism*; Oxford University Press: Oxford, England, 1961.

(31) Polverari, M.; van de Ven, T. G. M. *J. Phys. Chem.* **1996**, *100*, 13687.

(32) Graham, N. B.; Zulfiqar, M.; Nwachuku, N. E.; Rashid, A. *Polymer* **1989**, *30*, 528.

(33) Hammouda, B.; Ho, D. L.; Kline, S. *Macromolecules* **2004**, *37*, 6932.

(34) Tasaki, K. *J. Am. Chem. Soc.* **1996**, *118*, 8459.

(35) Holyst, R.; Bielejewska, A.; Szymanski, J.; Wilk, A.; Patkowski, A.; Gapinski, J.; Zywocinski, A.; Kalwarczyk, T.; Kalwarczyk, E.; Tabaka, M.; Ziebacza, N.; Wieczoreka, S. *Phys. Chem. Chem. Phys.* **2009**, *11*, 9025.

11958

dx.doi.org/10.1021/jp304569a | *J. Phys. Chem. B* 2012, 116, 11953−11958